Electronic Supplementary Material (ESI) for ChemComm.
This journal is © The Royal Society of Chemistry 2016

Electronic Supplementary information

Anodic performance of Black Phosphorus in Magnesium-ion Battery: The Significance of Mg-P Bond-synergy

Swastika Banerjee[a] and Swapan K. Pati*[a, b]

[a.] [†]New Chemistry Unit, [‡]Theoretical Sciences Unit
[b.] Jawaharlal Nehru Center for Advanced Scientific Research
[c.] Jakkur P. O., Bangalore 560064, India
[d.] *E-mail: swapan.jnc@gmail.com

Computational details

For all Density functional theory based calculations, Electron–ion interactions and electron exchange-correlation interactions have been taken into account by Projector-augmented-wave (PAW) potentials[1], and generalized gradient approximation (GGA)[2], respectively, as implemented in Vienna ab initio simulation package (VASP).[3] Plane wave cutoff of 600eVis used for all the calculations. The conjugate gradient algorithm is used to obtain the unstrained configuration. Atomic relaxation is performed until the change of total energy is less than 0.01 meV and all the forces on each atom are smaller than 0.01 eV/Å. *K*-point samplings of 7 × 7 × 1 (monolayer phosphorene) and 7 × 7 × 7 (bulk black phosphorus) are used for the structure relaxation.Denser meshes of 15 × 15 × 1 (monolayer) and 15 × 15 × 15 (bulk) are used to find the total energy and density of states and electron density. For the monolayer phosphorene, a vacuum space of 20 Å is placed between adjacent layers to avoid mirror interactions. Bulk black phosphorus is denoted as P, throughout the manuscript.

Regarding the size of the BP-anode, we would like to mention clearly that bulk form of black phosphorus is considered in this study, which is periodic along all three dimensions. To model different state-of-charge, a series of Mg_qP compositions with varying q values are

taken into account with 2×2×1 supercell with 32 P atoms. For 2D phosphorene, we have considered 2×2×1 supercell with 16 P atoms.

To understand the nature of the chemical bonding in M_qP composites, we have looked for the nature of the orbital overlap. Differential charge density has been computed by subtracting the superposition of the atomic charge densities from the total charge density in the crystal framework. *ab initio* Molecular Dynamics Simulations (NVT; 300 K) are based on quantum density functional theory using the same protocol as used for structural optimization.The length and time scales achieved in this study are 10 ps and 1fs, respectively. Nosé-Hoover type thermostat has been applied as temperature bath. To investigate the microstructure of crystalline materials, integrated radial pair distribution function has been calculated which allows local bonding analysis of multi-component mixtures. Representation of the Radial pair distribution function (RPDF) is based on a structural model using:

$$G(r) = \frac{1}{r}\sum_i \sum_j \frac{f(0)_i f(0)_j}{\langle f(0) \rangle^2} \delta(r - r_{ij}) - 4\pi r \rho_0 \quad (1)$$

Where the atomic RPDF G(r)= 4πr[ρ(r)- ρ_0], ρ_0 is average atomic number density, and ρ(r)is the atomic pair-density within the radial distance r. Here the f(0) s are the atomic formfactors evaluated at Q = 0 and Q denotes the momentum transfer. The simplified form of the so-called partial radial distribution functions, $g_{ij}(r)$, (when more than one chemical species are present) is:

$$g_{ij}(r) = \frac{dn_{ij}(r)}{4\pi r^2 dr \rho_i}; \rho_i = \frac{V}{N_i} \quad (2)$$

Where N_i represents the number density of atomic species, '*i*'. These functions give the density probability for an atom of the '*i*' species to have a neighbor of the '*j*' species at a given distance *r*.

Table T1. Calculated lattice parameters (lattice vectors: a, b and c are in Å and corresponding angles are in degree º) and volumes ($Å^3$) of the conventional unit cell of bulk black phosphorus with varying concentrations of stored Mg-ions are given.

	a(Å)	b (Å)	c (Å)	x (º)	y (º)	z (º)	Volume($Å^3$)
MgP	6.98	5.23	9.82	90.19	110.69	90.11	335.74
$Mg_{0.5}P$	4.21	6.71	11.45	69.19	68.40	51.12	230.86
$Mg_{0.25}P$	3.86	4.79	11.09	71.19	87.92	77.46	189.62
$Mg_{0.125}P$	3.25	4.71	11.55	72.30	90.07	89.98	168.32
$Mg_{0.06}P$	3.28	4.56	11.29	73.29	90.25	90.24	161.84
$Mg_{0.03}P$	3.26	4.51	11.38	72.65	90.00	90.00	160.83
$Mg_{0.02}P$	3.30	4.48	11.31	73.05	90.09	90.03	159.78
P_8	3.32	4.42	10.47	90.00	90.00	90.00	153.90

To visualize the bonding feature uponM-ion incorporation in α-phase, we have calculated the charge density difference using the following equation:

$$\Delta\rho\,(r) = \rho_{P+M}(r) - \rho_P(r) - \rho_M(r)$$

where $\rho_{P+M}(r)$ represents the charge density of M incorporated P-matrix (see Figure S1), $\rho_P(r)$ is the charge density of the P, and $\rho_M(r)$ is the charge density of isolated M atoms in the same position as in the total systems.Figure 4c, d(in main text) shows the charge density difference due to M atoms incorporation into P systems.

For the case of Li atom embedded in the interlayer space of P-matrix(Figure 4d), a net loss of electronic charge could be found above the Li. On the other hand, large gains in charge on P-atoms demonstrate the significant electronic transfer from Li atom to the neighboring P atoms, which indicates the high ionic bonding of the embedded Li atom. These findings are consistent with the previous Bader analysis,[4]and also confirm the high ionic interaction between Li and P.

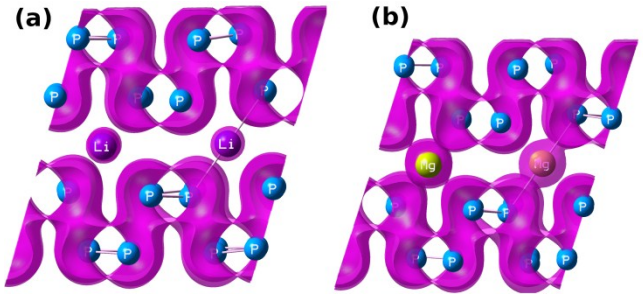

Figure S1. Total charge density (side view):(a) Li inserted into interlayer of P-anode; (b) Mg inserted into interlayer of P-anode for $M_{0.125}P$ composition.

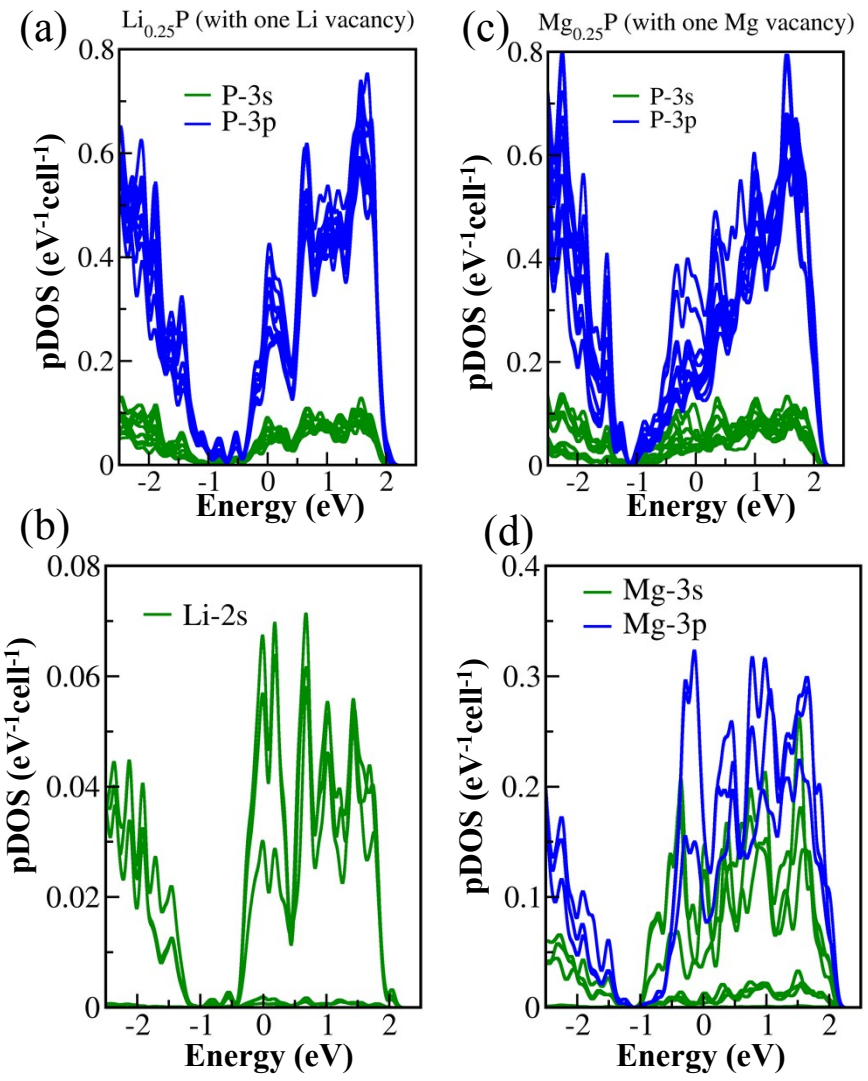

Figure S2. The projected density of states (PDOS) of M_qP (TR): (a, b) for M = Li; (c, d) for M = Mg.

For both the Li and Mg storage in α-phase, s and p states of phosphorus form separate s and p-bands (see Figure S2 a, c). However, the electronic states of Li and Mg ions (within P-matrix) exhibit different features. 3s-3p orbital mixing (see Figure S2 d) is found for Mg-ion, which participates in bonding with '3p' states of P-matrix, whereas, Li-s orbital (see Figure S2b) alone participates in bonding.

We estimate the percentage elongation or shrinkage of M-P bonds at TR on BS, for determination of the steric-instability (see Table T2).

Table T2. M(Li / Mg)-P bond distances(r in Å) at stable adsorption site (BS) as well as at the transition state configuration (TR) during hopping. The percentage elongation or shrinkage of M-P bonds at TR on BS (dr/r × 100 %) determines of the steric-instability at TR.

M in $M_{0.25}P$	a(Å)	a'(Å)	b (Å)	b'(Å)	c (Å)	c'(Å)
Mg(TR)	2.87	2.87	2.87	2.87475	2.46	2.46
Mg(BS)	2.72	2.72	2.72	2.70863	2.59	2.59
dr/r × 100 %	5.52%	5.89%	5.89%	6.28%	-4.64%	-4.64%
Li(TR)	2.83	2.83	2.83	2.83	2.39	2.39
Li(BS)	2.65	2.65	2.65	2.65	2.55	2.555
dr/r × 100 %	6.79%	6.79%	6.79%	6.79%	-6.27%	-6.27%

Table T3. The dispersive interaction energy per M (Li/Mg)-ions in α (q = 0.25), β (q = 0.50) and γ (q = 1.00) phases. The ratio between the number of Li-P and Mg-P pairs contributing to the dispersive interaction(N_{Li_qP}:N_{Mg_qP}) at different structural phases are given.

q	$E_{disp(Li_qP)}$: $E_{disp(Mg_qP)}$ 0 K (300 K)	N_{Li_qP} : N_{Mg_qP}
0.25	2.30 (1.50)	1.11 :1
0.50	2.39 (1.78)	1.13 :1
1.00	1.91 (1.55)	1.21 :1

[1] P. E. Blöchl, *Physical Review B* **1994**, *50*, 17953.
[2] J. P. Perdew, K. Burke, M. Ernzerhof, *Physical review letters* **1996**, *77*, 3865.
[3] aG. Kresse, J. Furthmüller, *Computational Materials Science* **1996**, *6*, 15-50;bG. Kresse, D. Joubert, *Physical Review B* **1999**, *59*, 1758.
[4] G.-C. Guo, D. Wang, X.-L. Wei, Q. Zhang, H. Liu, W.-M. Lau, L.-M. Liu, *The journal of physical chemistry letters* **2015**, *6*, 5002-5008.